Multidimensional Modelling of Cross-Beam Energy Transfer for Direct-Drive Inertial Confinement Fusion

(Hopefully soon to be Dr.) Philip W. X. Moloney

IMPERIAL

June 2024

Submitted in partial fulfilment of the requirements for the degree of
Doctor of Philosophy of Imperial College London

Department of Physics
Imperial College London
Prince Consort Road
London SW7 2AZ

Contents

List of Acronyms

Rad-MHD Radiative-Magnetohydrodynamics

MHD Magnetohydrodynamics

HEDP High Energy Density Physics

LPIs Laser-Plasma Instabilities

CBET Cross-Beam Energy Transfer

ICF Inertial Confinement Fusion

PiC Particle in Cell

EPW Electron Plasma Wave

IAW Ion Acoustic Wave

Inv-Brem Inverse-Bremsstrahlung

MCF Magnetic Confinement Fusion

VFP Vlasov-Fokker-Planck

EoS Equation of State

UV Ultraviolet

EMW Electro-Magnetic Wave

List of Tables

List of Figures

1 The Interaction of Light with Plasma

This chapter shall introduce theoretical background relevant to the work conducted in this thesis. The main focus of the work is centred on improving the laser modelling in the CHIMERA Radiative-Magnetohydrodynamics (Rad-MHD) code. Therefore, the theoretical framework for modelling both the plasma and the interaction of light with it is introduced.

Initially, the plasma state is defined and important length- and time-scales are provided in Sec. 1.1. The kinetic and fluid descriptions of plasma are introduced in Sec. 1.2 and the validity domain of each framework is discussed, with particular reference to typical conditions for laser-plasma interactions. Additional physics packages of the fluid code, CHIMERA, which are utilised in later chapters, are introduced. A model for kinetic heatflow is desirable in fluid codes which model laser-plasma interactions, therefore although CHIMERA does not have this capability, some basic theory of kinetic heatflow is highlighted.

An additional aim of the work was to include a Cross-Beam Energy Transfer (CBET) model into the new CHIMERA laser package. Laser-Plasma Instabilities (LPIs) such as CBET are multi-wave coupling phenomena, and therefore a basic description of waves in plasma is provided in Sec. 1.3. The dispersion relation of the light waves in plasma is also derived. Beginning with the full wave equation and then introducing successive assumptions which are broadly satisfied in typical laser-produced Inertial Confinement Fusion (ICF) plasmas, Sec. 1.4 derives the equations of ray-tracing. In Sec. **??** important absorption processes are then outlined, particularly Inverse-Bremsstrahlung (Inv-Brem), which is the dominant mechanism on the largest ICF facilities in the world today. Finally, the basic theory of LPIs is provided in Sec. 1.5, particularly CBET and its relevance for direct-drive ICF.

1.1 Basic Plasma Physics

As stated in Chap. **??**, thermonuclear fusion requires the fuel to exist at significant temperatures, which are well above ionisation energies. Therefore, the fuel configuration in these fusion experiments is a plasma. Formally, a plasma is defined as a quasi-neutral, ionised gas which exhibits collective behaviour [1]. The charged particles within a plasma interact via the long-range Coulomb force, and thus undergo many simultaneous interactions with the other particles. This leads to a variety of collective phenomena such as the plasma-waves described in Sec. 1.3. Quasineutrality of the plasma means that, when observed at a length-scale L, the plasma has no net charge,

$$\Sigma_\alpha q_\alpha N_\alpha = 0, \tag{1.1}$$

where N_α is the number of particles of species α, with charge q_α, in the cube with volume $V = L^3$. For a 'single-species' plasma[1] with average ionisation state Z, this implies,

$$n_e = Z n_i, \tag{1.2}$$

where n_e and n_i are the number densities of electrons and ions respectively.

Quasineutrality arises because the particles in the plasma are free to move due to forces they experience. Thus, if a local charge imbalance occurs, the electrons, which respond faster than the ion population due to their lower mass, move to rebalance this field and restore quasineutrality. This electron relocation to eliminate local electric fields is known as Debye-screening. The length scale below the electron population cannot effectively screen the charges sets the length scale of quasineutrality, and is known as the Debye-length,

$$\lambda_D^2 = \frac{\varepsilon_0 k_B T_e}{n_e e^2}, \tag{1.3}$$

where T_e is the electron temperature, ε_0 is the permittivity of free space, k_B is the Boltzmann constant and e is the electron charge. This screening can only occur if there is a large number of particles in the Debye sphere, $n_e L^3 \gg 1$.

The timescale of the charge relocation is of particular importance to the interaction of light with plasmas. Light waves are an oscillating electric field, which the charged particles in the plasma can respond to. If the particles are able to respond quickly enough, they can therefore influence the propagation of the light and ultimately force the plasma can become opaque to the propagating light wave. The oscillation timescale can be derived by considering a uniform assembly of quasineutral plasma and then displacing the electron population from the ions by a small distance δx along the x-axis. The electric field which develops within the plasma is thus,

$$E_x = \frac{n_e e \delta x}{\varepsilon_0}, \tag{1.4}$$

leading to a restoring force $F_x = -eE_x$ on each electron. Solving Newton's second Law demon-

[1] Single-species here means that there is only a single type of ion.

strates that, when thermal motion of the electron population is ignored[2], oscillations of the electrons occur at the 'plasma frequency',

$$\omega_p^2 = \frac{n_e e^2}{m_e \varepsilon_0}. \tag{1.5}$$

If forcing oscillations occur at a frequency which is lower than ω_p, then the electrons move rapidly enough to nullify the field. Consider light with frequency ω, which is incident normal to a plasma density gradient Because $\omega_p \propto n_e$, the light is able to propagate until it reaches the density where $\omega = \omega_p$, which is known as the critical density,

$$n_{\text{cr}} = \frac{m_e \varepsilon_0 \omega^2}{e^2}. \tag{1.6}$$

After reaching the critical density, the field of the light decays exponentially as an evanescent wave, but cannot propagate.

1.2 The Kinetic and Fluid Formulations

Idealised computational modelling of a plasma state would solve the long-range electromagnetic interaction between every pair of particles at all times. However, this very rapidly becomes intractable due to the large number N of particles and the $\mathcal{O}(N^2)$ scaling of interactions to solve. Reduced frameworks must thus be devised with which to analyse and predict the behaviour of the plasma state. Plasmas are divided into two broad classifications. When in local thermal equilibrium, the plasma is often described as 'thermal' and the fluid formulation is an adequate description. There are numerous situations when this is not true however, for instance if a particular subset of particles is heated at a rate, which is much faster than thermalising collision timescales. In this case, the subset of the system is described as 'non-thermal' or 'kinetic'. The fluid formulation becomes an inadequate description and higher fidelity, kinetic tools must be used to describe the evolution of the system.

When a kinetic description of a plasma is required, the distribution function, $f_\alpha(\mathbf{x}, \mathbf{v}, t)$ is used to describe the state of particle species α. It provides a statistical description of the number density of particles, which inhabit a phase-space, $\mathbf{x}$-$\mathbf{v}$, at time t. If the system evolves on a timescale much lower than the collision time and plasma length scales are lower than the collisional mean free-path, then these collisions between particles act to locally relax the distribution function toward a Maxwellian,

$$f_{\alpha,\text{Max.}}(v) = n_\alpha \left(\frac{1}{2\pi v_{T\alpha}^2} \right)^{1.5} e^{-\left[v/(\sqrt{2} v_{T\alpha})\right]^2}, \tag{1.7}$$

where $v_{T\alpha} = \sqrt{k_B T_\alpha / m_\alpha}$ is the thermal speed of the species with temperature and mass T_α and m_α, respectively. The fraction outside the exponential is set such the integral over velocity space yields the number density of the species. Typically, for bulk of the target con-

[2] Inclusion of thermal motion leads to pressure, which acts as a restoring force, and yields the dispersion relation for an EPW.

figuration throughout a laser-produced ICF implosion, the assumption of a Maxwellian distribution is close to accurate, although there are several notable exceptions. For instance, DT fusion products have energies much higher than thermal energies and are also monoenergetic. LPIs also generate energetic electron populations which are able to range through the implosion due to their low collisionality [2]. Additionally, laser-heated plasmas typically exhibit steep density and temperature gradients near the ablation surface, such that collisions, and therefore collision processes such as transport of thermal energy, do not act locally [3]. When performing fluid simulations of ICF experiments, accurate modelling of these phenomena requires specific non-local modelling techniques.

1.2.1 The Vlasov Equation

The evolution of the distribution function for each species individually, is described by the Vlasov equation,

$$\frac{\partial f_\alpha}{\partial t} + \mathbf{v}.\nabla_x f_\alpha + \frac{q_\alpha}{m_\alpha}(\mathbf{E} + \mathbf{v}\times\mathbf{B}).\nabla_v f_\alpha = \left(\frac{\partial f_\alpha}{\partial t}\right)_{\text{collisions}} + \left(\frac{\partial f_\alpha}{\partial t}\right)_{\text{external}}, \tag{1.8}$$

where q_α is the charge of the species, **E** and **B** are the macroscopic electric and magnetic fields[3], respectively, and ∇_x and ∇_v are gradients with respect to position and velocity coordinates respectively [4]. The equation describes the conservation of phase-space particle density. The collision operator on the right-hand side of Eq. 1.8 describes the action of microscopic fields, which arise due to the random motion of the charged plasma particles. External forces, for example gravity, are also accounted for in the second right-hand side term. Evolution of the macroscopic fields is governed by Maxwell's equations,

$$\nabla.\mathbf{E} = \frac{\rho_{\text{charge}}}{\varepsilon_0}, \tag{1.9}$$

$$\nabla.\mathbf{B} = 0, \tag{1.10}$$

$$\nabla\times\mathbf{E} = -\frac{\partial\mathbf{B}}{\partial t}, \tag{1.11}$$

$$\nabla\times\mathbf{B} = \mu_0\varepsilon_0\frac{\partial\mathbf{E}}{\partial t} + \mu_0\mathbf{J}, \tag{1.12}$$

where μ_0 is the permeability of free space, ρ_{charge} is the charge density, **J** is the current density and $\nabla \equiv \nabla_x$. In the general case with three spatial dimensions, Eq. 1.8 is seven dimensional and evolves on small spatial and temporal scales. Therefore, it is typically too expensive to solve in its entirety for the relatively long times and large spatial scales of an entire ICF implosion. Solution methods to the Vlasov equation include Vlasov-Fokker-Planck (VFP) codes, which discretise the 6-D phase space of Eq. 1.8 and evolve the state forward in time [5]. The velocity space can be either directly discretised [6], or expanded in spherical harmonics [7]. Alternatively, the distribution function can be approximated by Monte Carlo techniques, which is done in Particle in Cell (PiC) codes [8]

[3]Macroscopic here means on a scale larger than the Debye length.

1.2.2 The Fluid Equations

Due to the expense of the Vlasov equation, the assumption of local thermodynamic equilibrium can be used to derive the fluid equations. By inserting Eq. 1.7 into Eq. 1.8, multiplying each side of the equation by functions of $\mathbf{v}$ and integrating over velocity space, the fluid equations can be derived. This process is known as taking moments of the Vlasov equation. A moment of the Vlasov equation at order n of $\mathbf{v}$ yields an equation which depends upon the $n+1$ moment. A solvable system of equations thus requires an external closure. The inviscid hydrodynamic equations[4] are obtained from $n = [0,1,2]$ moments,

$$\left[\frac{\partial}{\partial t} + \mathbf{u}_\alpha.\nabla\right]\rho_\alpha + \rho_\alpha \nabla.\mathbf{u}_\alpha = 0, \tag{1.13}$$

$$\rho_\alpha \left[\frac{\partial}{\partial t} + \mathbf{u}_\alpha.\nabla\right]\mathbf{u}_\alpha = -\nabla P_\alpha + \mathbf{F}_{\alpha,L} + \mathbf{F}_{\alpha,\text{ext.}} + \mathbf{F}_{\alpha,\text{col.}}, \tag{1.14}$$

$$\left[\frac{\partial}{\partial t} + \mathbf{u}_\alpha.\nabla\right]U_\alpha + (U_\alpha + P_\alpha)\nabla.\mathbf{u}_\alpha = -\nabla.\mathbf{q}_\alpha + Q_{\alpha,\text{ext.}} + Q_{\alpha,\text{col.}}, \tag{1.15}$$

where ρ_α is the mass density of species α, $\mathbf{u}_\alpha$ is the fluid velocity, U_α is the internal energy, P_α is the isotropic pressure, $\mathbf{F}_{\alpha,L} = n_\alpha q_\alpha(\mathbf{E} + \mathbf{u}_\alpha \times \mathbf{B})$ is the Lorentz, $\mathbf{F}_{\alpha,\text{ext.}}$ is external forcing, $\mathbf{F}_{\alpha,\text{col.}}$ is collisional forcing, $\mathbf{q}_\alpha$ is the heat flux, $Q_{\alpha,\text{ext.}}$ is external heating or cooling and $Q_{\alpha,\text{col.}}$ is collisional heating or cooling [9]. A closure relation for the plasma pressure can be obtained from an Equation of State (EoS), such as the ideal gas law, which relates pressure to density, temperature and energy density. The heat flux can be obtained from Fourier's law,

$$\mathbf{q}_\alpha = -\kappa \nabla T_\alpha, \tag{1.16}$$

where the thermal conductivity, κ, is obtained from local transport theory [10, 11].

The single-fluid, two temperature hydrodynamic equations can be obtained by assuming quasineutrality ($Zn_i = n_e = n$), the electron mass is negligible to the ion mass ($m_i \gg m_e$) and modelling only a single ion-species[5]. The populations will therefore be co-moving, and it follows that,

$$\rho \equiv m_i n_i + m_e n_e \approx m_i n, \tag{1.17}$$

$$\mathbf{u} \equiv \frac{(\rho_i \mathbf{u}_i + \rho_e \mathbf{u}_e)}{\rho} \approx \mathbf{u}_i, \tag{1.18}$$

where the fluid density, ρ, and velocity, $\mathbf{u}$, have been defined. Noting also that collisions within a fluid will not affect their net momentum and that collisional forces between the electron and ion will cancel, the fluid equations for electrons and ions can be added to obtain

[4] Note that since the velocity dependence has been integrated out, all variables are now only functions of $\mathbf{x}$.

[5] When multiple ion-species compose the plasma, *e.g.* for CH ablator or DT fuel, then the average ion mass (by number density) must be used and frictional forces/ temperature separation between ion species ignored.

the single-fluid, two temperature equations,

$$\left[\frac{\partial}{\partial t}+\mathbf{u}.\nabla\right]\rho+\rho\nabla.\mathbf{u}=0, \tag{1.19}$$

$$\rho\left[\frac{\partial}{\partial t}+\mathbf{u}.\nabla\right]\mathbf{u}=-\nabla P+\mathbf{F}_L, \tag{1.20}$$

$$\left[\frac{\partial}{\partial t}+\mathbf{u}.\nabla\right]U_e+(U_e+P_e)\nabla.\mathbf{u}=-\nabla.\mathbf{q_e}+Q_{e,\text{ext.}}+Q_{e,\text{col.}}, \tag{1.21}$$

$$\left[\frac{\partial}{\partial t}+\mathbf{u}.\nabla\right]U_i+(U_i+P_i)\nabla.\mathbf{u}=-\nabla.\mathbf{q_i}+Q_{i,\text{ext.}}+Q_{i,\text{col.}}, \tag{1.22}$$

where the total pressure is defined, $P = P_e + P_i$, the external forcing has been dropped, and equilibration between the electron and ion temperatures occurs via the collisional heating terms $Q_{\alpha,\text{col.}}$. By defining the current from electron motion in the frame of the plasma, $\mathbf{J} = -n_e e(\mathbf{u}_e - \mathbf{u})$ and utilising quasineutrality, the Lorentz force term in the single fluid approximation,

$$\mathbf{F}_L = \mathbf{J}\times\mathbf{B}. \tag{1.23}$$

The CHIMERA code solves the two-temperature, single fluid equations. In the absence of magnetic fields, the Lorentz force term goes to zero. Macroscopic magnetic fields can be included under the extended-Magnetohydrodynamics (MHD) framework, and their evolution and effect on plasma transport and dynamics is discussed in Sec. 1.2.4. Further details of the numerical solution to the fluid equations can be found in Refs. [12, 13, 14, 15, 16, 17]. Additional physics packages are included by calculating contributions to the external forces and heating. For example, the non-thermal fusion products are modelled by a Monte Carlo treatment, which collide with the bulk plasma and thus deposit energy which contributes to the electron and ion $Q_{\alpha,\text{ext.}}$ [18]. The additional physics packages which are utilised in the subsequent work presented in this manuscript are discussed briefly below.

1.2.3 Radiation Transport

For this section, a distinction between coherent, approximately visible or Ultraviolet (UV) wavelength laser radiation, and higher frequency ($\omega \gg \omega_p$) x-ray radiation is drawn. The former is the main focus of Chap. **??**. It refracts significantly in coronal plasma density gradients and radiation at this wavelength is not significantly re-emitted by the thermal plasma. In contrast, the latter does not significantly refract and is re-emitted by in ICF plasma conditions. The latter is accounted for numerically in CHIMERA by a radiation transport algorithm, which is cursively described here.

In addition to driving the implosion of indirect-drive ICF experiments, x-ray radiation is also significant in a wide array of laser-driven High Energy Density Physics (HEDP) physics experiments. For example, the hot coronal plasma in direct-drive radiates a significant amount of energy as thermal Bremsstrahlung emission. This both lowers the coronal temperatures, reducing the thermal conduction drive efficiency and also preheats the fuel, making it harder to compress. Radiation acts both as a source and sink of energy, as it is radiated and emitted by the material, depending on the plasma conditions and the atomic properties. Thermal emission is wavelength dependent and atomic transitions create sharp resonances of emissivity and opacity in wavelength space. Therefore, the radiation-transport algorithm must be discretised in wavelength, depending on the properties of the material and the plasma conditions.

The radiative transfer equation describes the propagation, absorption, emission and scattering of photons with matter,

$$\frac{\partial I_\nu}{\partial t} + c\hat{\Omega}.\nabla i_\nu = \left(\frac{\partial I_\nu}{\partial t}\right)_{\text{collisions}} + \left(\frac{\partial I_\nu}{\partial t}\right)_{\text{source}}, \tag{1.24}$$

where c is the speed of light in vacuum, I_ν is the spectrally resolved radiation intensity, $\hat{\Omega}$ is the photon direction of travel [9]. The left-hand side describes the advection of radiation at speed c and the first and second terms on the right-hand side describe collisions between matter and photons, and emission or absorption of photons by the matter respectively. Eq. 1.24 is seven dimensional, and therefore is typically highly expensive to solve, so approximations are often employed to make solutions more tractable. In analogy to derivation of the fluid equations from the Vlasov equation, angular moments of Eq. 1.24 can be taken to reduce the dimensionality of the problem. This also leads to a requirement for a closure relation, and the approach taken in CHIMERA is to use the $P_{1/3}$ closure, which works well for highly isotropic radiation fields [19]. More detail of the CHIMERA implementation is provided in Refs. [20, 21].

1.2.4 Magnetohydrodynamics

The method used to evolve macroscopic magnetic fields and their impact upon the plasma dynamics and transport is discussed in this section. Magnetic fields are able to alter the evolution of the plasma state via the Lorentz force in Eq. 1.20 and by altering the conductivities in Eq. 1.16. The relative importance of magnetisation can typically be broadly assessed by calculating dimensionless numbers. For instance, the plasma β describes the ratio of thermal pressure to the magnetic pressure[6],

$$\beta = \frac{2\mu_0 P}{|\mathbf{B}|^2}. \tag{1.25}$$

This gives an order of magnitude estimate for when it is necessary to include the Lorentz force in the momentum equation, *i.e.* for high beta plasmas, thermal pressure dominates over magnetic pressure. Similarly, the Hall parameter, $\omega_\alpha \tau_\alpha$, describes the ratio of the gyrofrequency to the collision frequency for a species, α. For example, the electron Hall parameter,

$$\omega_e \tau_e = \frac{e|\mathbf{B}|}{m_e} \frac{3\sqrt{m_e}(k_B T_e)^{1.5}}{4\sqrt{2\pi} e^4 Z^2 n_i \ln\Lambda}, \tag{1.26}$$

where $\ln\Lambda$ is the Coulomb logarithm, which is an important parameter for collisional phenomena that is related to the impact parameter of collisions [22, 23, 24]. When $\omega_\alpha \tau_\alpha \sim 1$,

[6]Using Ampère's law with $(\partial \mathbf{E}/\partial t) \ll c^2$, the Lorentz force in Eq, 1.23 can be recast as the sum of magnetic pressure and tension [16].

then collisional phenomena, such as thermal conduction, are significantly affected by the magnetic field.

The evolution of the magnetic field is governed by Faraday's law (Eq. 1.11) and the electric field by Ampère's law (Eq. 1.12). This is not a closed system of equations due to the appearance of **J** in Ampère's law however, and therefore an additional equation is required to evolve the fields. This can be derived from the momentum equations for ions and electrons, Eq. 1.14 [15]. In the limit of no electron inertia, the left-hand side of Eq. 1.14 is zero, leading to the 'generalised Ohm's law',

$$\mathbf{E} = -\mathbf{u}\times\mathbf{B} + \frac{\mathbf{J}\times\mathbf{B}}{n_e e} - \frac{\nabla P_e}{n_e e} + \frac{1}{n_e e}\left(\frac{\overline{\alpha}.\mathbf{J}}{n_e e} - n_e\overline{\beta}.\nabla T_e\right), \tag{1.27}$$

where $\overline{\alpha}$ and $\overline{\beta}$ are transport coefficient tensors, the precise form of which is described in, for example, Ref. [16]. Taking the curl of Eq. 1.27 and combining with Faraday's law yields the magnetic induction equation,

$$\frac{\partial\mathbf{B}}{\partial t} = \nabla\times\left(\mathbf{u}\times\mathbf{B} - \frac{\mathbf{J}\times\mathbf{B}}{n_e e} + \frac{\nabla P_e}{n_e e} - \frac{\overline{\alpha}.\mathbf{J}}{n_e^2 e^2} + \frac{\overline{\beta}.\nabla T_e}{e}\right). \tag{1.28}$$

Each term on the right-hand side of the Eq. 1.28 is ascribed a physical affect. The first term describes advection of the field with the movement of the plasma. When this term dominates, the 'ideal MHD' framework is obtained, in which the field is said to be frozen-in to the flow. Ideal MHD can often be applied in fields such as space physics [25, 26] and Magnetic Confinement Fusion (MCF) [27], where many phenomena featuring highly conductive plasmas are well described by this limit. In order from the second term on the right-hand side, the subsequent terms are related to, the Hall effect (collisionless advection of field with current), the Biermann effect (generation of field), resistive phenomena and thermoelectric phenomena. The non-ideal terms of relevance to the work conducted in this thesis are discussed below.

1.2.4.1 Resistive MHD

When only the first term and the resistive term from Eq. 1.28 are significant (and using a simple form for the transport coefficient, $\overline{\alpha}$), then the induction equation can be written,

$$\frac{\partial\mathbf{B}}{\partial t} = \nabla\times(\mathbf{u}\times\mathbf{B}) - \nabla\times\left(\frac{\eta}{\mu_0}\nabla\times\mathbf{B}\right), \tag{1.29}$$

where η is the resistivity of the plasma [15]. As already discussed, the first term describes advection of the plasma with the fluid, whereas the second term describes resistive diffusion of the plasma. This effect moves **B** from regions of high- to low-field, via the damping of currents due to collisions between electrons and ions. Resistive diffusion can lead to phenomena such as magnetic reconnection [28, 29]. The relative importance of these two terms is described by the magnetic Reynolds number, which is the ratio field advection to diffusion,

$$R_m = \frac{\mu_0 |\mathbf{u}| L}{\eta}, \tag{1.30}$$

where L is the characteristic length scale of the system.

1.2.4.2 The Nernst Effect

The Nernst effect arises from the thermoelectric term in Eq. 1.28, and makes a contribution to the field induction,

$$\left(\frac{\partial \mathbf{B}}{\partial t}\right)_{\text{Nernst}} = \nabla \times \left(-\frac{\beta_\wedge}{e|\mathbf{B}|} \nabla T_e \times \mathbf{B}\right), \tag{1.31}$$

where $\beta_\wedge$ is a transport coefficient. This contribution looks like an advection of the field in the direction of $-\nabla T_e$ with a velocity,

$$\mathbf{v}_N = -\frac{\beta_\wedge}{e|\mathbf{B}|} \nabla T_e. \tag{1.32}$$

Nernst-advection of magnetic field is often of particular importance to magnetised HEDP experiments, acting to move field down temperature gradients, even when the plasma is highly conductive [30, 13]. As this is a collisional phenomenon, it is most important in regions where the electron Hall parameter is low, $\omega_e \tau_e \ll 1$.

1.2.4.3 Magnetised Thermal Conduction

Magnetic fields can affect collisional transport anisotropically by forcing particles to gyrate around field lines, which changes their collisional behaviour anisotropically. Because the Lorentz force does not affect particle motion in the direction parallel to field lines, transport along the direction, $\hat{\mathbf{b}} = \mathbf{B}/|\mathbf{B}|$, is unaffected by magnetisation. However, the gyration around field lines restricts transport in the perpendicular direction, compared to the parallel direction. Local transport analysis of the heat flux demonstrates that the electron thermal conduction heatflow can be expanded,

$$\mathbf{q}_e = -\kappa_\parallel \hat{\mathbf{b}} \left(\hat{\mathbf{b}} . \nabla T_e\right) - \kappa_\perp \hat{\mathbf{b}} \times \left(\nabla T_e \times \hat{\mathbf{b}}\right) - \kappa_\wedge \hat{\mathbf{b}} \times \nabla T_e, \tag{1.33}$$

where the $\kappa_\parallel$ term describes thermal conduction parallel to the field, $\kappa_\perp$ perpendicular to the field and $\kappa_\wedge$ perpendicular to the field and the temperature gradient [11]. The wedge term, $\kappa_\wedge$, describes 'Righi-Leduc' heatflow, which occurs along isotherms. Considering the first two terms, when unmagnetised, $\kappa_\parallel = \kappa_\perp$ and conduction is isotropic. As the magnetisation increases, however, $\kappa_\perp$ decreases with respect to $\kappa_\parallel$, for example, $\kappa_\perp / \kappa_\parallel \sim 1$ at $\omega_e \tau_e = 1$, which anisotropises the thermal conduction.

1.2.5 Kinetic Heatflow

While the CHIMERA implementation of thermal transport is simply to use the local limit described in Eq. 1.16, this is not always a valid approximation in laser produced plasmas. When laser-heating is applied to a plasma, laser energy is transferred to the electron population mostly by Inv-Brem, as is described in Sec. **??**, heating the electron fluid to significant temperatures. For laser-solid interactions, this often results in sharp temperature and density gradients in the conduction zone, where the thermal energy of the hot corona is transported via thermal conduction to an ablation surface. To assess whether local transport theory is valid, the Knudsen number is a convenient parameter which compares the mean free path of electrons, λ_{mfp} to the length scale of the gradient, L. Specifically, the Knudsen number is defined,

$$\mathrm{Kn} = \frac{\lambda_{\mathrm{mfp}}}{L} = \frac{3(k_B^2 T_e^2)}{4\sqrt{2\pi}e^4 Z^2 n_i \ln \Lambda L}, \tag{1.34}$$

and transport effects, become significantly non-local when Kn ~ 0.1, which is often observed for high-power laser solid conduction zones [31]. Physically, more energetic particles within a plasma are less collisional and also play a more significant role in heat flux because it is obtained a higher order moment quantity than density or fluid velocity. Therefore, the fast heat carrying particles in the tail of the distribution function are able to range through longer length scales and preheat the fuel more than a local treatment would predict. Although not included within CHIMERA, models for non-local transport exist, which can be included in fluid models, such as SNB [32, 33, 34, 35], Fast-VFP [36] and RKM [37]. They obtain an improved heat flux estimate, **q**, which accounts for non-local conduction effects such including pre-heat, ad can be included in the fluid framework. Implementation of one of these models into CHIMERA could significantly improve the modelling capability for simulations involving laser-solid interactions, including direct-drive calculations.

1.3 Waves in Fluid Plasma

LPIs are a class of multi-wave coupling phenomena that occur when a light wave excites additional plasma-waves. Therefore, understanding LPIs requires some background theoretical knowledge of the relevant waves. In the absence of a macroscopic magnetic field, three classes of wave can propagate in a plasma: the IAW, the EPW and the EMW, *i.e.* a light wave. This section shall describe the basic theory of these waves and provide dispersion relations for their propagation. The treatment provided in this section assumes that the plasma acts as a fluid. For a full kinetic treatment, the reader is referred to the work of Michel in Ref. **??**, from which many of the following relations are also obtained.

1.3.1 Plasmas as a Dielectric Medium

Freely moving particles in a plasma are able to respond to external electric fields by relocating, which reduces the size of the field that the plasma sees. In others words plasma are dielectric, and it is therefore convenient to define the permittivity of the plasma in analogy to solutions of Maxwell's equations in matter. The dielectric displacement vector is defined,

$$\mathbf{D} = \varepsilon_0 \varepsilon \mathbf{E}, \tag{1.35}$$

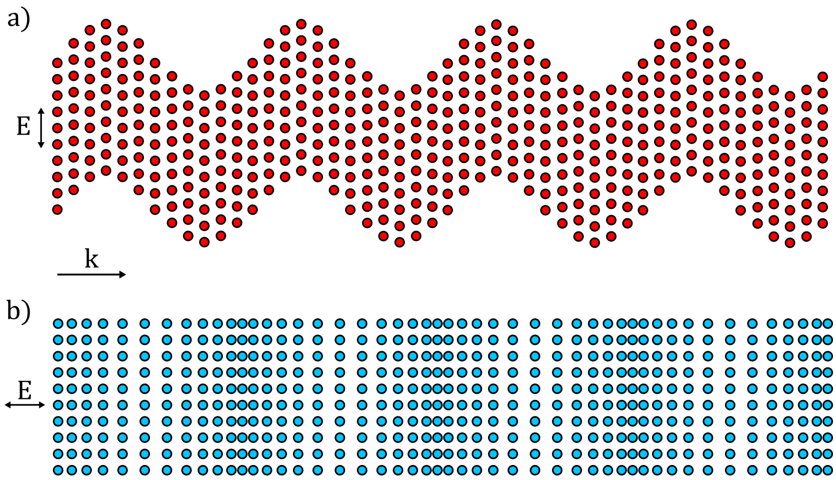

Figure 1.1: Particle motion in a) transverse and b) longitudinal plasma waves. This diagram was adapted from Ref. [38].

where ε is the permittivity of the plasma[7]. Defining the electrical conductivity, σ, such that $\mathbf{J} = \sigma\mathbf{E}$ it can be shown that the permittivity takes the form,

$$\varepsilon = 1 + i\frac{\sigma}{\varepsilon_0\omega} \equiv 1 + \chi, \tag{1.36}$$

where the dielectric susceptibility, χ, has been introduced [38]. The permittivity and susceptibility represent the plasma response to applied fields. In general, each species within a plasma contributes separately to the susceptibility, such that $\chi = \sum_\alpha \chi_\alpha$, where χ_α are the contributions from electrons and the individual ion species within the plasma.

In order to describe waves, the plasma of the plasma must be described in observable variables. Here, the plasma is treated as a fluid, and is allowed to respond linearly to the applied fields. An initially uniform, stationary plasma in equilibrium is considered with a number density for each species, $n_{\alpha 0}$. Assuming an ideal gas equation of state and plasma conditions, the plasma response is described by a velocity ($\delta\mathbf{v}_\alpha$) and density (δn_α) perturbation, because the temperature perturbation is proportional to the density perturbation [38]. Linearising, we seek a solution to the following plasma response,

$$n_\alpha(\mathbf{x}, t) = n_{\alpha 0} + \delta n_\alpha(\mathbf{x}, t), \tag{1.37}$$

$$\mathbf{v}_\alpha(\mathbf{x}, t) = \mathbf{v}_{\alpha 0} + \delta\mathbf{v}_\alpha(\mathbf{x}, t) \quad = 0 + \delta\mathbf{v}_\alpha(\mathbf{x}, t), \tag{1.38}$$

$$\mathbf{E}(\mathbf{x}, t) = \mathbf{E}_0 + \delta\mathbf{E}(\mathbf{x}, t) \quad = 0 + \delta\mathbf{E}(\mathbf{x}, t), \tag{1.39}$$

$$\mathbf{B}(\mathbf{x}, t) = \mathbf{B}_0 + \delta\mathbf{B}(\mathbf{x}, t) \quad = 0 + \delta\mathbf{B}(\mathbf{x}, t), \tag{1.40}$$

$$\tag{1.41}$$

where the subscript 0 quantities are (constant) the equilibrium values and $\delta\mathbf{E} = \mathbf{E}$ and $\delta\mathbf{B} = \mathbf{B}$ are the applied fields. Inserting the linearised equations for each species into Eq. 1.19 and

[7]Outside of plasma physics, the displacement vector is usually defined $\mathbf{D} = \varepsilon\mathbf{E} = \varepsilon_0\varepsilon_r$ and ε_r is the 'relative' permittivity.

Eq. 1.20 it can be shown [38],

$$\frac{\delta n_\alpha}{n_{\alpha 0}} = \frac{\mathbf{k}.\delta\mathbf{v}_\alpha}{\omega}, \tag{1.42}$$

$$\omega\delta\mathbf{v}_\alpha = \gamma_\alpha v_{T\alpha}^2 \frac{\delta n_\alpha}{n_{\alpha 0}}\mathbf{k} + i\frac{q_\alpha}{m_\alpha}\mathbf{E}, \tag{1.43}$$

where γ_α is the adiabatic index, ω is the conjugate variable of time, t, from a Laplace transform and $\mathbf{k}$ is the conjugate variable of space, $\mathbf{x}$, from a Fourier transform. These equations can then be combined to relate δn_α and $\delta\mathbf{v}_\alpha$ to $\mathbf{E}$,

$$\left[\omega^2 - \gamma_\alpha v_{T\alpha}^2 k^2\right]\frac{\delta n_\alpha}{n_{\alpha 0}} = i\frac{q_\alpha}{m_\alpha}\mathbf{k}.\mathbf{E}, \tag{1.44}$$

$$\left[\omega^2 - \gamma_\alpha v_{T\alpha}^2 \mathbf{k}(\mathbf{k}.)\right]\delta\mathbf{v}_\alpha = i\frac{q_\alpha\omega}{m_\alpha}\mathbf{k}.\mathbf{E}. \tag{1.45}$$

Assuming a plane wave of the form $\mathbf{E} \propto \exp\left[i\left(\mathbf{k}.\mathbf{x} - \omega t\right)\right]$, we identify $\mathbf{k}$ as the wavenumber and ω as the angular frequency. Using the Ansatz that waves can either be transverse ($\mathbf{k}.\mathbf{E} = 0$) or longitudinal ($\mathbf{k} \times \mathbf{E} = 0$), dispersion relations in the fluid regime can be obtained for admissible solutions using these equations. Fig. 1.1.a and Fig. 1.1.b plot the motion of particles from each of these varieties.

1.3.2 Electromagnetic Waves

Firstly, the transverse wave solution shall be obtained, which is an EMW propagating in the plasma. Inserting the transverse wave Ansatz ($\mathbf{k}.\mathbf{E} = 0$) into Eq. 1.45 demonstrates that $\mathbf{k}.\delta\mathbf{v}_\alpha = 0$, and therefore $\delta\mathbf{v}_\alpha = \delta\mathbf{v}_{\alpha\perp}$. The transformed equation for the conservation of momentum, Eq. 1.43 yields,

$$\delta\mathbf{v}_{\alpha\perp} - i\frac{q_\alpha}{m_\alpha\omega}\mathbf{E}, \tag{1.46}$$

which demonstrates that under the Lorentz force of the field, the particles undergo oscillatory 'quiver' motion. The quiver velocity of the ions is ignored because $m_i \gg m_e$ and therefore the ions are considered as a static background compared to the electron oscillations. Therefore, the linearised current is only from the electron motion, $\sum_\alpha \delta\mathbf{J}_\alpha \sim \delta\mathbf{J}_e = -en_{e0}\delta\mathbf{v}_e = \sigma\mathbf{E}$. Utilising the definition of the permittivity from Eq. 1.36, the plasma response to an EMW is obtained,

$$\varepsilon = 1 - \frac{\omega_p^2}{\omega^2} = 1 - \frac{n_{e0}}{n_{\mathrm{cr}}}, \tag{1.47}$$

$$\chi = -\frac{\omega_p^2}{\omega^2}, \tag{1.48}$$

where the plasma frequency, defined previously in Eq. 1.5, has emerged.

A dispersion relation can also be obtained by utilising Maxwell's equations. Taking the curl of Faraday's law (Eq. 1.11) and combining this with Ampère's law (Eq. 1.12) to eliminate $\mathbf{B}$ yields,

$$\left[\partial_t^2 - c^2\nabla^2 + c^2\nabla(\nabla.)\right]\mathbf{E} = -\frac{1}{\varepsilon_0}\partial_t\mathbf{J}. \tag{1.49}$$

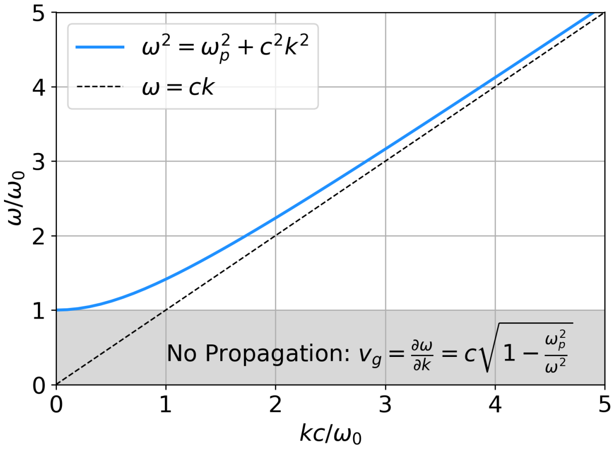

Figure 1.2: The dispersion relation for an EMW propagating in a plasma. For $\omega < \omega_p$, the oscillatory plane wave Ansatz turns into a decaying evanescent wave, thus the wave does propagate.

Inserting a plane wave Ansatz for $\mathbf{E}$ and inserting Eq. 1.47 to eliminate $\mathbf{J}$, the dispersion relation and wave equation for an EMW are obtained,

$$\omega^2 - \omega_p^2 - c^2k^2 = 0, \tag{1.50}$$

$$\left(\partial_t^2 + \omega_{pe}^2 - c^2\nabla^2\right)\mathbf{E}(\mathbf{x}, t) = 0, \tag{1.51}$$

which is plotted in Fig. 1.2. For $\omega < \omega_p$, Eq. 1.50 demonstrates that k becomes imaginary and therefore the plane wave Ansatz turns into a non-propagating, exponentially decaying evanescent wave. The phase v_ϕ and group v_g velocities of the light are,

$$v_\phi = \frac{w}{k} = \frac{c}{\sqrt{\varepsilon}}, \tag{1.52}$$

$$v_g = \frac{\partial w}{\partial k} = \sqrt{\varepsilon}c, \tag{1.53}$$

which defines the refractive index of plasma, $n_{\mathrm{ref}} = \sqrt{\varepsilon} = \sqrt{1 - n_e/n_{\mathrm{cr}}}$. Note that $\sqrt{\varepsilon} < 1$ so $v_\phi > c$. However, the group velocity, which is the speed that information travels, remains subluminal. Additionally, a wave equation for

1.3.3 Plasma Waves

Two propagating longitudinal wave can exist in an unmagnetised plasma, an EPW, which are oscillations of the electron fluid on a timescale which is too fast for the ions to respond and an IAW, which is a slower, joint oscillation of the electron and ion fluid. The inertia of the EPW and IAW are set by the electron and ion masses respectively. Electron pressure drives the EPW, whereas both fluids contribute to the IAW pressure, depending on the ionisation level of the plasma. Fig. 1.3 illustrates particle motion in each wave. Dispersion relations can be obtained similarly to the EMW method from Sec. 1.3.2. By first inserting the longitudinal a)

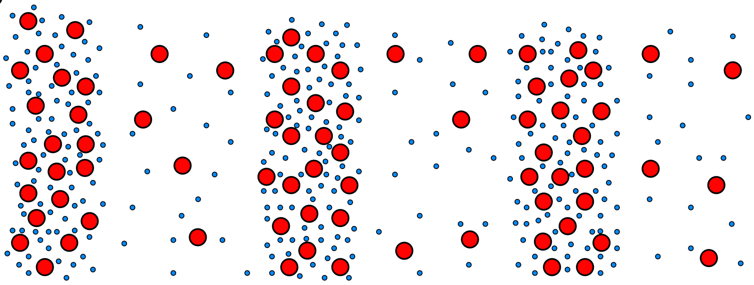

b)

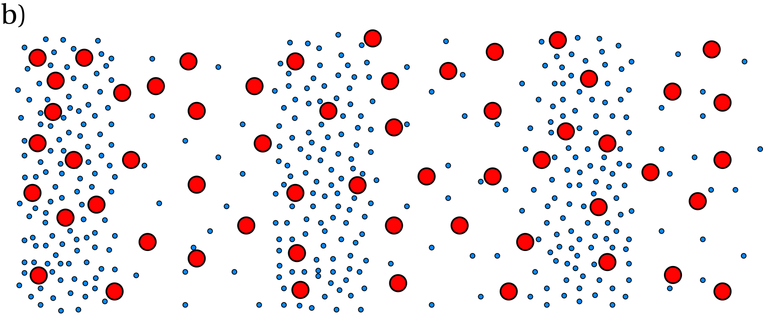

Figure 1.3: Illustration of electron (small blue circle) and ion (large red circle) motion in a) an IAW and b) an EPW.

Ansatz ($\mathbf{k} \times \mathbf{E} = 0$) into Eq. 1.45 to obtain the particle motion in a longitudinal wave,

$$\delta \mathbf{v}_\alpha = i \frac{q_\alpha \omega}{m_\alpha} \frac{\mathbf{E}}{\omega^2 - \gamma_\alpha v_{T\alpha}^2 k^2}. \tag{1.54}$$

Unlike the EMW, we make no assumptions yet about which species contribute to the current, and thus the general form of the conductivity for longitudinal waves includes contributions from all species,

$$\sigma = i\omega\varepsilon_0 \sum_\alpha \frac{\omega_{p\alpha}^2}{\omega^2 - \gamma_\alpha v_{T\alpha}^2 k^2}, \tag{1.55}$$

which yields the longitudinal wave permittivity and equivalently susceptibility,

$$\varepsilon = 1 + \sum_\alpha \chi_\alpha, \tag{1.56}$$

$$\chi_\alpha = -\frac{\omega_{p\alpha}^2}{\omega^2 - \gamma_\alpha v_{T\alpha}^2 k^2}. \tag{1.57}$$

Inserting the plane wave Ansatz into 1.49 and using Eq. 1.56 to eliminate $\mathbf{J}$ yields the generalised dispersion relation for longitudinal waves in a plasma,

$$\varepsilon \mathbf{E} = 0. \tag{1.58}$$

Further use of an Ansatz can be utilised to obtain a specific description of a particular plasma wave. Note that unlike transverse waves, where $\delta n_\alpha = 0$, which is seen by inserting $\mathbf{k}.\mathbf{E}$ into Eq. 1.44, longitudinal waves do give rise to a density perturbation, which heuristically can be understood by looking at Fig. 1.1. This leads to an electric field within the plasma, which is important for damping.

The longitudinal susceptibility (Eq. 1.57) has a pole at $\omega^2 = \gamma_\alpha v_{T\alpha}^2 k^2$, suggesting unbounded growth of the wave when its phase velocity is close to the thermal velocity of the species, α. This does not occur in actuality however, due to a process known as Landau damping, which is a resonant exchange of energy from the wave to particles. When the phase velocity of the wave approaches this resonance, particles with velocity just below the group velocity, $\mathbf{v} \lesssim \mathbf{v}_\phi$, are trapped in the potential created by the charge separation and accelerated. This transfers energy from the wave to the particles and thus prevents unbounded growth of the density perturbation.

1.3.3.1 Electron Plasma Waves

Firstly the EPW shall be considered. These are fast oscillations of the electron fluid such that the heavier ions do not respond on the oscillation timescale. To arrive at the dispersion relation, the assumption that the phase velocity is much faster than the electron thermal velocity is made, such that the wave can freely propagate without experiencing strong Landau damping, $w/k \gg v_{Te}$. This assumption also yields $\lambda \gg v_{Te}/\omega$, which states that electrons travelling at the thermal velocity will not move a significant portion of the wavelength, λ, in one oscillation. Temperature equilibration is thus limited throughout the wave, which means that there is no heat flux and such the electron fluid is adiabatic. An adiabatic fluid has $\gamma_e = 3$, which is equivalent to a single degree of freedom in the motion. Finally, assuming that the ions are slow due to their large mass, and thus do not contribute to the permittivity[8]. By using these assumptions in the generalised dispersion relation for longitudinal plasma waves, Eq. 1.58, the dispersion relation for the EPW is obtained,

$$\omega^2 = \omega_{pe}^2 + 3k^2 v_{Te}^2. \tag{1.59}$$

Just as for light waves, EPW cannot propagate at $\omega \geq \omega_{pe}$. The phase and group velocity of the wave are obtained from this dispersion relation,

$$v_\phi = \frac{w}{k} = v_{Te}\frac{\sqrt{1+3k^2\lambda_D^2}}{k\lambda_D}, \tag{1.60}$$

$$v_g = \frac{\partial w}{\partial k} = 3v_{Te}\frac{k\lambda_D}{\sqrt{1+3k^2\lambda_D^2}}. \tag{1.61}$$

1.3.3.2 Ion Acoustic Waves

The IAW is of particular importance to the work conducted in this thesis, because it is the wave that mediates the energy exchange between light waves in CBET. To obtain the dispersion relation for this wave, the phase velocity of the wave is assumed to be much greater than the thermal velocity of the ions, but much less than the electron thermal velocity[9]. Using the

[8] Explicitly for the EPW, $\omega/k \gg v_{Te} \gg v_{Ti}$ and thus $|\chi_e| \gg |\chi_i|$

[9] For the IAW, $v_{Ti} \ll \omega/k \ll v_{Te}$.

same logic as the electrons, the ion fluid is assumed to be adiabatic, so $\gamma_i = 3$. The electrons, however, move much faster than the wave. Therefore, they are able to equilibrate their temperature across the wave in a single oscillation, and are taken to be isothermal ($\gamma_e = 1$). When inserted into Eq. 1.58, these assumptions yield the dispersion relation,

$$\omega^2 = \frac{k^2}{1+k^2\lambda_D^2}\frac{ZT_e}{m_i} + 3k^2 v_{Ti}^2. \tag{1.62}$$

For oscillation wavelengths much larger than the Debye length, $k\lambda_D \ll 1$, this simplifies to,

$$\omega \approx c_s k, \tag{1.63}$$

where the sound speed is defined,

$$c_s = \sqrt{\frac{Zk_BT_e + 3k_BT_i}{m_i}}. \tag{1.64}$$

The phase and group velocity of the light are thus simply c_s in this limit, so the wave is non-dispersive.

Commonly in ICF, plasmas are composed of multiple ion species, for instance the ablator of OMEGA targets is commonly composed of a CH plastic or SiO_2 glass shell. The IAW properties are typically greatly altered due to the additional susceptibility contributions from each species. This leads to multiple IAW modes with distinct speeds and damping. Denoting the 'heavy' and 'light' ion species as h and l respectively, a fast ion mode exists when the phase velocity is greater than both ion thermal velocities,

$$v_{Th} \leq v_{Tl} \ll v_{\phi,\mathrm{fast}} \ll v_{Te}. \tag{1.65}$$

A fast mode is also observed when only the heavy ion species are slower than the phase velocity,

$$v_{Th} \ll v_{\phi,\mathrm{slow}} \ll v_{Tl} \ll v_{Te}. \tag{1.66}$$

This is of particular relevance to the work in this manuscript, since CBET in direct-drive typically occurs in multi-ion ablators, and it is moderated by an energy exchange via an IAW. Therefore, for example, different wave phenomena can affect the growth and saturation of energy transfer and must be accurately accounted for in computational modelling. This leads to the different CBET treatments, described in Sec. **??**.

1.4 Propagation and Absorption of Light in a Plasma

This section shall describe light propagating and absorption through plasma in the regime of typical ICF conditions. Typically, sub-critical laser-driven ICF plasmas can be treated as a linear medium and intensity of the light is sufficiently modest that it does not directly alter the refractive index of the plasma. By making the WKB approximation, which is that over a wavelength the plasma may be treated as uniform, the equations of ray-tracing are derived.

Ray-tracing is the tool used to model lasers in the SOLAS model, described in Chap. **??**. Absorption processes, which are important to energy deposition in laser-drive ICF are then introduced, particularly collisional absorption, otherwise known as Inv-Brem. An absorption per unit length for Inv-Brem is provided, which is suitable for integration along ray trajectories.

1.4.1 WKB Approximation

Laser-driven plasmas are heated and expand, leadig to density gradients in the region where the light propagates. The propagation path of the light through this plasma is governed by the refractive index, or equivalently permittivity, $\varepsilon = n_{\text{ref}}^2 = 1 - n_e/n_{\text{cr}}$. Thus, light refracts in plasmas with a density gradient. Here, a description of light propagation through a non-uniform plasma is obtained, in the limit that the plasma density does not vary significantly over the wavelength of the oscillation. It is convenient to work with vector potentials, $\mathbf{B} = \nabla \times \mathbf{A}$ and $\mathbf{E} = -\partial_t \mathbf{A}$[10], rather than electric field for laser-plasma waves. This is because electric fields can describe longitudinal and trasverse waves, whereas the vector potential is purely for transverse oscillations and as such cannot describe plasma waves. Using the vector potential, the EMW wave equation, Eq. 1.51, can be rederived from Maxwell's equations,

$$\left(\partial_t^2 + \omega_{pe}^2 - c^2\nabla^2\right)\mathbf{a} = 0, \tag{1.67}$$

where the normalised vector potential is defined,

$$\mathbf{a} = \frac{e}{mc}\mathbf{A}. \tag{1.68}$$

If the wave propagates normally up a plasma density gradient (aligned with z), polarisation of the wave can be ignored by rotational symmetry and a solution can be souhgt of the form,

$$a(z,t) = \frac{1}{2} f(z) a_0 e^{-i\omega_0 t} + c.c., \tag{1.69}$$

where ω_0 is the vacuum angular frequency, a_0 is the oscillation amplitude, $c.c.$ is the complex conjugate and $f(z)$ is the spatial dependene of the oscillation. In this limit, the WKB (Wentzel, Kramers, Brillouin) approximation can be used to find a solution for $f(z)$.

Inserting Eq. 1.69 into the wave equation, Eq. 1.67, yields the Helmholtz equation,

$$\left[\partial_z^2 + \varepsilon(z) k_0^2\right] f(z) = 0, \tag{1.70}$$

where $k_0 = \omega_0/c$ is the vacuum wavenumber. This describes the steady state propagation of light through a plasma, which is defined by the permittivity, ε. The WKB method assumes that spatial variations of the medium are much larger than the wavelength, *i.e.* $\lambda_0 = 2\pi/k_0 \ll 1/|\nabla\varepsilon|$. An Ansatz is used [38],

$$f(z) = e^{ik_0\varphi(z)}, \tag{1.71}$$

[10] Note that the Coulomb gauge has been used here, $\nabla.\mathbf{A} = 0$, otherwise $\mathbf{E} = -\partial_t\mathbf{A} - \nabla\phi$, where ϕ is the scalar potential.

where φ is a series expansion [39],

$$\varphi(z) = k_0 \left[S_0(z) + \frac{S_1(z)}{i k_0} + \frac{S_2(z)}{(i k_0)^2} + \dots \right], \tag{1.72}$$

which is valid so long as the expansion parameter is large, $k_0 = \omega_0 / c \gg 1/|\nabla\varepsilon|$.

By combining Eqs. 1.70, 1.71 and 1.72 and keeping only the dominant, $\mathcal{O}(k_0^2)$ terms, the expression for the first order expansion term is obtained,

$$S_0(z) = \pm \int_0^z \sqrt{\varepsilon(z)}\, \mathrm{d}z. \tag{1.73}$$

If only this term is kept and there is a uniform plasma (therefore ε is constant), then a plane wave propagating solution is obtained for the field,

$$a(z,t) = \frac{a_0}{2} \exp\left[i(\pm k_0 z - \omega_0 t)\right]. \tag{1.74}$$

If the next order terms, $\mathcal{O}(k_0^1)$, are collected and equated, then the following expression is retrieved,

$$S_1(z) = i \ln\left(\varepsilon^{1/4}\right) + k_0 \varphi_0, \tag{1.75}$$

where $k_0\varphi_0$ is an integration constant, identified as the initial phase of the light. This returns an expression for the light field [38],

$$a(z,t) = \frac{1}{2} \frac{a_0}{\varepsilon^{1/4}} \exp\left[\pm i \int_0^z k(z) \mathrm{d}z - i\omega_0 t + i k_0 \varphi_0 \right] + c.c, \tag{1.76}$$

where $k(z) = \sqrt{\varepsilon(z)}\, k_0$. The $\varepsilon^{1/4}$ term outside the exponential leads to higher field in regions of the plasma with higher densities and is known as 'field-swelling.' It occurs due to the reduced group velocity of light at lower ε values, resulting in a pile up of field as light propagates up a density gradient. The validity condition of the WKB solution in Eq. 1.76 can be demonstrated by mandating that the $\mathcal{O}(k_0^0)$ order terms from the expansion are much smaller than the $\mathcal{O}(k_0^1)$ terms. This leads to the validity domain (for the normally incident light considered here),

$$\frac{|\nabla\varepsilon|}{\varepsilon} \ll k, \tag{1.77}$$

where, stated again for emaphasis, $k = \sqrt{\varepsilon}\, k_0$. In other words, the lengthscale L associated with $\nabla\varepsilon$ must be far larger than the oscillation wavelength $\lambda = 2\pi/(k_0\sqrt{\varepsilon})$. This condition is violated either for plasmas with extreme density gradients, or in a narrow region near the critical surface, where the oscillation wavelength grows to infinity.

1.4.2 Ray Tracing

The WKB approximation correctly captures the behaviour of light, apart from a narrow region near the wave turning point. Ray-tracing is a technique, which provides a framework to integrate the WKB solution along the trajectory of the light, at discrete points on an initial pahse front. This turns out to be a highly useful tool for numerical implemnetation of laser modeling. Starting from the Helmholtz equation, now generalised to multiple dimensions [39],

$$\left[\nabla^2 + \varepsilon(\mathbf{x})k_0^2\right] a(\mathbf{x}) = 0, \tag{1.78}$$

a solution is sort of the form,

$$a(\mathbf{x}) = A(\mathbf{x})e^{ik_0\varphi(\mathbf{x})}, \tag{1.79}$$

where going from 1-D→3-D, we have made the change $f(z) \to A(\mathbf{x})$, where $A(\mathbf{x})$ is now the 'ray-amplitude.' Similarly to Sec. 1.4.1, $\varphi(\mathbf{x})$ is expanded, and the Ansatz is inserted into the Helmholtz equation, which returns the following equations:

$$\left(\nabla\varphi(\mathbf{x})\right)^2 = \varepsilon(\mathbf{x}), \tag{1.80}$$

$$2\left(\nabla A(\mathbf{x}).\nabla\varphi(\mathbf{x})\right) + A(\mathbf{x})\nabla^2\varphi(\mathbf{x}) = 0, \tag{1.81}$$

where Eq. 1.80 is known as the Eikonal equation, and Eq. 1.81 is known as the transport equation. So far, this is simply a multi-dimesional corolorary of the same procedure that was followed in Sec. 1.4.1.

Give equations, interpretations and validity. State can be used for any kind of wave where valid. Say how and why used for direct drive and typical frozen plasma assumption.

Talking about validity region, give extra bits can solve like ray amplitude.

1.4.3 Inv Brem

Introduce all bits to get NRL formaularly equation. Talk about Langdon as well.

1.4.4 Resonance Absorption

Introduce

1.4.5 ICF Relevant Absorption comparison

Say inv brem goes up relatively at larger scales and shorter wavelengths. Prefered to resonance absorption because bulk population gets energy. Therefore use frequency tripled light.

1.5 Laser Plasma instabilities

1.5.1 Ponderamotive Force

Introduce and say why it happens roughly.

1.5.2 Three-Wave Coupling

Give the general picture, i.e. ponderamotive, perturbation, driven plasma wave. Give momentum and energy conservation. List all types seeded by an EMW.

1.5.3 Cross-Beam Energy Transfer

Derive something to an appropriate level of detail. Talk about how it is in frame of plasma, flow velocities change this, mach 1 surface etc. Give general picture, i.e. sidescatter and backscatter and what it does in ICF.

1.5.3.1 Linear Gain Theory

Say that we use this for raytracing. Assume uniform plasma and can solve plasma response either by linearising fluid or kinetic equations.

1.5.3.2 Effect of Polarisation

Say that LPIs are affected by polarisation via ponderatmotive beat. Only parallel polarisations interact. Important on OMEGA due to polarisation smoothing, leads to mode-1.

1.5.3.3 Langdon Effect on CBET

Say that Langdon affects cbet. Reduced model to alter linear gain. Could potentially explain why indirect ICF models require a clamp.

1.5.4 Mitigation of Laser Plasma Instabilities

Say its coherence spatially, temporally and spectrally, so break this to stop LPIs. Mention stud pulses and say zooming for CBET.

Mainstream approach is bandwidth. Talk about studies showing that bandwidth should mitigate CBET. Talk about experimental progress eg FLUX laser at LLE.

1.6 Summary

Summarise that introduced descriptions of plasmas, particularly fluid framework solved by CHIMERA. Talked about waves in plasmas and their physical interpareatations. Talked about how light propagates, assumptions etc, used for raytracing in next section. LPIs, particularly CBET, modelling it is focus of next chapter.

Appendices

Bibliography

[1] Francis F. Chen. *Introduction to Plasma Physics and Controlled Fusion*. Third edition, corrected publication. Cham: Springer, 2018. ISBN: 978-3-319-22308-7.

[2] D. Barlow et al. “Role of Hot Electrons in Shock Ignition Constrained by Experiment at the National Ignition Facility”. In: *Physics of Plasmas* 29.8 (Aug. 2022), p. 082704. ISSN: 1070-664X, 1089-7674. DOI: 10.1063/5.0097080.

[3] E. M. Epperlein and R. W. Short. “A Practical Nonlocal Model for Electron Heat Transport in Laser Plasmas”. In: *Physics of Fluids B: Plasma Physics* 3.11 (Nov. 1991), pp. 3092–3098. ISSN: 0899-8221. DOI: 10.1063/1.859789.

[4] J. A. Bittencourt. *Fundamentals of Plasma Physics*. 3rd ed. New York: Springer, 2004. ISBN: 978-0-387-20975-3.

[5] A.G.R. Thomas et al. “A Review of Vlasov–Fokker–Planck Numerical Modeling of Inertial Confinement Fusion Plasma”. In: *Journal of Computational Physics* 231.3 (Feb. 2012), pp. 1051–1079. ISSN: 00219991. DOI: 10.1016/j.jcp.2011.09.028.

[6] W.T. Taitano et al. “An Eulerian Vlasov-Fokker–Planck Algorithm for Spherical Implosion Simulations of Inertial Confinement Fusion Capsules”. In: *Computer Physics Communications* 263 (June 2021), p. 107861. ISSN: 00104655. DOI: 10.1016/j.cpc.2021.107861.

[7] R.J. Kingham and A.R. Bell. “An Implicit Vlasov–Fokker–Planck Code to Model Non-Local Electron Transport in 2-D with Magnetic Fields”. In: *Journal of Computational Physics* 194.1 (Feb. 2004), pp. 1–34. ISSN: 00219991. DOI: 10.1016/j.jcp.2003.08.017.

[8] T D Arber et al. “Contemporary Particle-in-Cell Approach to Laser-Plasma Modelling”. In: *Plasma Physics and Controlled Fusion* 57.11 (Nov. 2015), p. 113001. ISSN: 0741-3335, 1361-6587. DOI: 10.1088/0741-3335/57/11/113001.

[9] John I. Castor. *Radiation Hydrodynamics*. 1st ed. Cambridge University Press, Sept. 2004. ISBN: 978-0-521-83309-7 978-0-521-54062-9 978-0-511-53618-2. DOI: 10.1017/CBO9780511536182.

[10] S. I. Braginskii. “Transport Processes in a Plasma”. In: *Reviews of Plasma Physics* 1 (Jan. 1965), p. 205. URL: https://ui.adsabs.harvard.edu/abs/1965RvPP....1..205B (visited on 09/16/2024).

[11] E. M. Epperlein and M. G. Haines. “Plasma Transport Coefficients in a Magnetic Field by Direct Numerical Solution of the Fokker–Planck Equation”. In: *The Physics of Fluids* 29.4 (Apr. 1986), pp. 1029–1041. ISSN: 0031-9171. DOI: 10.1063/1.865901.

[12] J. P. Chittenden et al. "Signatures of Asymmetry in Neutron Spectra and Images Predicted by Three-Dimensional Radiation Hydrodynamics Simulations of Indirect Drive Implosions". In: *Physics of Plasmas* 23.5 (May 2016), p. 052708. ISSN: 1070-664X. DOI: 10.1063/1.4949523.

[13] C. A. Walsh. "Extended Magneto-Hydrodynamic Effects in Indirect Drive Inertial Confinement Fusion Experiments". PhD thesis. London: Imperial College London, 2018.

[14] Aidan Crilly. "Simulation of Nuclear Observables in Inertial Confinement Fusion Experiments". PhD thesis. London: Imperial College London, Apr. 2020. URL: https://inspirehep.net/literature/1850910 (visited on 09/05/2024).

[15] Griffin Farrow. "Extended Magnetohydrodynamic Effects in Z-Pinch Plasmas". PhD thesis. London: Imperial College London, Aug. 2023.

[16] Sam Thomas Jack O'Neill. "Modelling Ignition and Burn in Pre-magnetised Inertial Confinement Fusion Experiments". PhD thesis. London: Imperial College London, Dec. 2023.

[17] Nikita Chaturvedi. "Simulating Radiatively Cooled Pulsed-Power Driven Systems Using Static Mesh Refinement". PhD thesis. London: Imperial College London, Dec. 2024.

[18] J.K. Tong et al. "Burn Regimes in the Hydrodynamic Scaling of Perturbed Inertial Confinement Fusion Hotspots". In: *Nuclear Fusion* 59.8 (Aug. 2019), p. 086015. ISSN: 0029-5515, 1741-4326. DOI: 10.1088/1741-4326/ab22d4.

[19] J. E. Morel. "Diffusion-Limit Asymptotics of the Transport Equation, the P1/3 Equations, and Two Flux-Limited Diffusion Theories". In: *Journal of Quantitative Spectroscopy and Radiative Transfer* 65 (Feb. 2000), pp. 769–778. ISSN: 0022-4073. DOI: 10.1016/S0022-4073(99)00148-X.

[20] Chris Jennings. "Radiation Transport Effects in Wire Array Z-Pinches and Magneto-Hydrodynamic Modelling Techniques". PhD thesis. London: Imperial College London, 2005.

[21] K. McGlinchey. "Radiation-Hydrodynamics Simulations of the Impact of Instabilities and Asymmetries of Inertial Confinement Fusion". PhD thesis. London: Imperial College London, 2017.

[22] T. S. Ramazanov and S. K. Kodanova. "Coulomb Logarithm of a Nonideal Plasma". In: *Physics of Plasmas* 8.11 (Nov. 2001), pp. 5049–5050. ISSN: 1070-664X, 1089-7674. DOI: 10.1063/1.1407820.

[23] S. K. Kodanova et al. "Investigation of Coulomb Logarithm and Relaxation Processes in Dense Plasma on the Basis of Effective Potentials". In: *Contributions to Plasma Physics* 55.2-3 (Feb. 2015), pp. 271–276. ISSN: 0863-1042, 1521-3986. DOI: 10.1002/ctpp.201400094.

[24] Chengliang Lin et al. “Temperature Relaxation and Generalized Coulomb Logarithm in Two-Temperature Dense Plasmas Relevant to Inertial Confinement Fusion Implosions”. In: *Nuclear Fusion* 63.10 (Oct. 2023), p. 106005. ISSN: 0029-5515, 1741-4326. DOI: `10.1088/1741-4326/acee96`.

[25] George K. Parks. “Why Space Physics Needs to Go beyond the MHD Box”. In: *Space Science Reviews* 113.1/2 (2004), pp. 97–121. ISSN: 0038-6308. DOI: `10.1023/b:spac.0000042941.14372.9b`.

[26] M. Mathioudakis et al. “Alfvén Waves in the Solar Atmosphere: From Theory to Observations”. In: *Space Science Reviews* 175.1-4 (June 2013), pp. 1–27. ISSN: 0038-6308, 1572-9672. DOI: `10.1007/s11214-012-9944-7`.

[27] Allen H. Boozer. “Equations for Studies of Feedback Stabilization”. In: *Physics of Plasmas* 5.9 (Sept. 1998), pp. 3350–3357. ISSN: 1070-664X, 1089-7674. DOI: `10.1063/1.873048`.

[28] M. M. Kuznetsova et al. “Multiscale Modeling of Magnetospheric Reconnection”. In: *Journal of Geophysical Research: Space Physics* 112.A10 (Oct. 2007). ISSN: 0148-0227. DOI: `10.1029/2007ja012316`.

[29] Judit Pérez-Coll Jiménez et al. “The Role of Resistivity on the Efficiency of Magnetic Reconnection in MHD”. In: *Journal of Geophysical Research: Space Physics* 127.6 (June 2022). ISSN: 2169-9380, 2169-9402. DOI: `10.1029/2021ja030134`.

[30] S. A. Slutz et al. “Pulsed-Power-Driven Cylindrical Liner Implosions of Laser Preheated Fuel Magnetized with an Axial Field”. In: *Physics of Plasmas* 17.5 (May 2010). ISSN: 1070-664X, 1089-7674. DOI: `10.1063/1.3333505`.

[31] W Q Yuan et al. “Space-Time Dependent Non-Local Thermal Transport Effects on Laser Ablation Dynamics in Inertial Confinement Fusion”. In: *Plasma Physics and Controlled Fusion* 66.4 (Apr. 2024), p. 045023. ISSN: 0741-3335, 1361-6587. DOI: `10.1088/1361-6587/ad27f1`.

[32] G. P. Schurtz et al. “A Nonlocal Electron Conduction Model for Multidimensional Radiation Hydrodynamics Codes”. In: *Physics of Plasmas* 7.10 (Oct. 2000), pp. 4238–4249. ISSN: 1070-664X, 1089-7674. DOI: `10.1063/1.1289512`.

[33] Ph. D. Nicolaï et al. “A Practical Nonlocal Model for Heat Transport in Magnetized Laser Plasmas”. In: *Physics of Plasmas* 13.3 (Mar. 2006), p. 032701. ISSN: 1070-664X, 1089-7674. DOI: `10.1063/1.2179392`.

[34] Duc Cao et al. “Improved Non-Local Electron Thermal Transport Model for Two-Dimensional Radiation Hydrodynamics Simulations”. In: *Physics of Plasmas* 22.8 (Aug. 2015), p. 082308. ISSN: 1070-664X, 1089-7674. DOI: `10.1063/1.4928445`.

[35] M. Sherlock et al. “A Comparison of Non-Local Electron Transport Models for Laser-Plasmas Relevant to Inertial Confinement Fusion”. In: *Physics of Plasmas* 24.8 (Aug. 2017), p. 082706. ISSN: 1070-664X, 1089-7674. DOI: `10.1063/1.4986095`.

[36] Anthony R Bell and Mark Sherlock. “The *Fast* VFP Code for Solution of the Vlasov-Fokker-Planck Equation”. In: *Plasma Physics and Controlled Fusion* (Jan. 2024). ISSN: 0741-3335, 1361-6587. DOI: `10.1088/1361-6587/ad2278`.

[37] N T Mitchell et al. “A Reduced Kinetic Method for Investigating Non-Local Ion Heat Transport in Ideal Multi-Species Plasmas”. In: *Plasma Physics and Controlled Fusion* 66.7 (July 2024), p. 075005. ISSN: 0741-3335, 1361-6587. DOI: `10.1088/1361-6587/ad4740`.

[38] Pierre Michel. *Introduction to Laser-Plasma Interactions*. Graduate Texts in Physics. Cham: Springer, 2023. ISBN: 978-3-031-23423-1 978-3-031-23426-2.

[39] A. Colaïtis et al. “Towards Modeling of Nonlinear Laser-Plasma Interactions with Hydrocodes: The Thick-Ray Approach”. In: *Physical Review E* 89.3 (Mar. 2014), p. 033101. DOI: `10.1103/PhysRevE.89.033101`.

Permissions